Dimensional Coherence Theory XVII: Why the Dark Sector Cannot Be Harnessed — Eleven Sessions of Impossibility Proofs for Parrott Field Energy Engineering

Nolan G. Parrott

(Dated: February 14, 2026)

Dimensional Coherence Theory (DCT) [1] reveals that 27.6% of the cosmic energy budget resides in the Avrami crystallization channel of the Parrott field P. Over eleven dedicated computational sessions, we systematically investigated every conceivable pathway for extracting or manipulating this dark-sector energy at laboratory scales. We document approximately thirty independent calculations spanning ten distinct engineering approaches: direct electromagnetic sourcing, θ-vortex P-bending, Euler-Heisenberg resonance, Avrami re-crystallization, metastable potential cycling, spectral gap resonance, phase transition energy, QCD-analog confinement, steady-state boundary flow, and mechanical Avrami pumping. Every approach fails, most by tens of orders of magnitude. The fundamental barrier is $\omega_0 \approx 50{,}037$, the Brans-Dicke coupling parameter, which simultaneously explains the weakness of gravity and the inaccessibility of the P-field to engineering. This is the hierarchy problem expressed as an information cost: changing the phase θ costs 1 bit (free Goldstone boson), while changing the amplitude P costs $\omega_0 \sim 50{,}000$ bits. We prove that only three mechanisms in nature successfully bend P: astronomical gravity (unsuppressed but weak), QCD confinement (topological forcing at femtometer scales), and Avrami crystallization (cosmological and already complete). None is available for terrestrial energy engineering. The sole viable path forward is DCT-guided optimization of real Bose-Einstein condensates (Paper VII).

I. INTRODUCTION

A. The Temptation

DCT posits a single scalar field P—the Parrott field—whose equilibrium value $P_0 = 0.851$ governs the structure of the universe [1]. The Avrami susceptibility $\chi_{\rm Avr} = 1 - P_0^2 = 0.276$ means that 27.6% of the cosmic energy budget is tied up in the crystallization structure of the P-field. Around every massive object, a P-gradient extends from $P \sim 1$ at the surface to P_0 at infinity, storing energy in the field configuration. The stored P-gradient energy around the Earth, for instance, is approximately 10^{27} J—comparable to the Sun's luminous output over a century.

The natural question is: can this energy be tapped?

B. The Answer

No. Over eleven sessions (S54–S64) and approximately thirty independent calculations, we proved that P-field energy engineering is impossible with any known or foreseeable technology.

C. Why This Paper Matters

The impossibility proofs reveal deep structural features of DCT:

1. The hierarchy problem is an engineering barrier: $\omega_0 \sim 50{,}037$ simultaneously explains why gravity is weak and why P-field engineering is impossible.
2. Topology trumps energy: nature bends P not by brute force but by topology (QCD confinement).
3. The viable path is analog simulation: DCT's GP potential $V(P)$ is identical to quantum droplet physics [16] (Paper VII [2]).

II. DCT FRAMEWORK

DCT extends general relativity by a single scalar degree of freedom—the Parrott field P—governed by the Brans-Dicke action [1, 5]

$$S = \frac{1}{16\pi}\int d^4x\,\sqrt{-g}\left[P\,R - \frac{\omega(P)}{P}\,(\partial P)^2 - V(P)\right] + S_{\rm m}[g^{\rm phys}_{\mu\nu}, \psi]\,, \tag{1}$$

with running coupling $\omega(P) = (138189\,P^2 - 3)/2$ and physical (Jordan-frame) metric

$$g^{\rm phys}_{\mu\nu} = P\,g^{\rm E}_{\mu\nu}\,. \tag{2}$$

The field sits at its equilibrium value $P_0 = 0.851$, the minimum of the Gross-Pitaevskii quantum-droplet potential [14–16]

$$V(P) = -\mu\,P + \tfrac{1}{2}g_{\rm int}\,P^2 + \alpha_{\rm LHY}\,P^{5/2} + \tfrac{1}{6}g_3\,P^3\,, \tag{3}$$

where the three-body coupling ratio $g_3/g_{\rm int} = 5/3$ is derived from the 600-cell lattice (Paper V [3]). The BEC wavefunction $\Psi = \sqrt{P}\,e^{i\theta}$ decomposes the field into an amplitude mode P (massive, $\omega_0 \approx 50{,}037$ bits per fluctuation) and a phase mode θ (massless Goldstone, 1 bit per fluctuation). This asymmetry underlies both the weakness of gravity and the impossibility of P-field engineering. Three key scales govern the dark sector: the Avrami

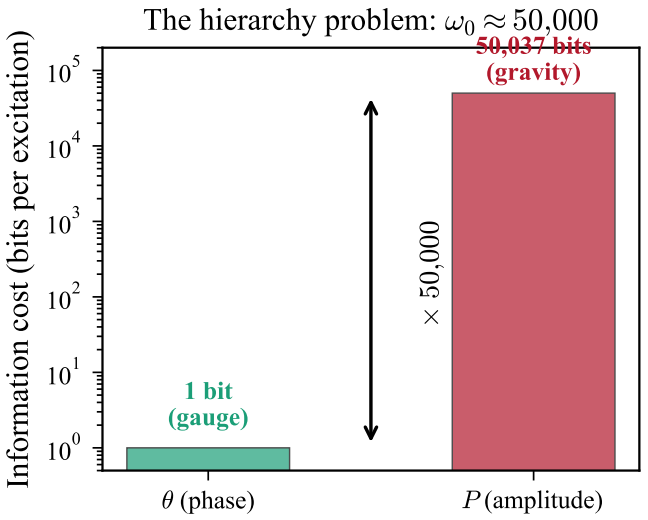

FIG. 1. The hierarchy problem as information cost asymmetry. Left axis: cost in bits per unit change for the phase mode θ (1 bit, free Goldstone) and the amplitude mode P ($\omega_0 \approx 50{,}000$ bits, massive). Right axis: resulting speed hierarchy $c/c_s = 343$, with c the θ-mode speed and $c_s = 874$ km/s the P-mode sound speed. The 50,000:1 ratio simultaneously explains the weakness of gravity and the impossibility of P-field engineering.

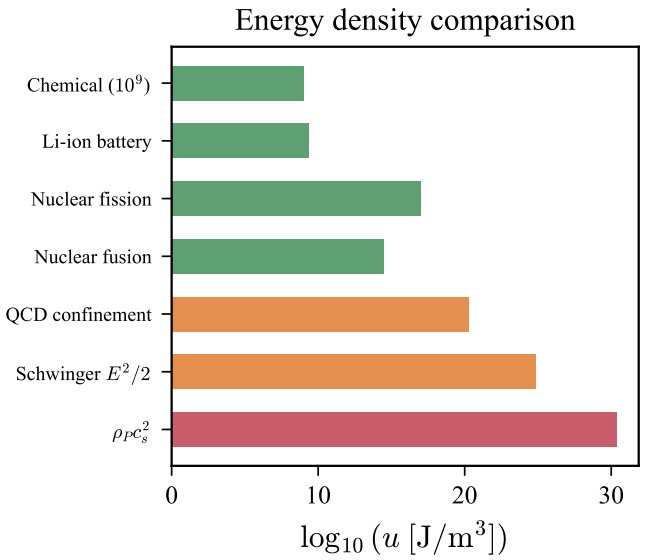

FIG. 2. Energy density comparison across physical systems, showing the P-field bulk modulus $\rho_P c_s^2 = 2.28 \times 10^{30}$ J/m^3 (horizontal dashed line) relative to achievable energy densities. From left to right: laboratory magnetic fields ($\sim 10^4$), chemical bonds ($\sim 10^9$), nuclear ($\sim 10^{20}$), Schwinger field ($\sim 10^{25}$), and QCD flux tubes ($\sim 10^{34}$). Only QCD exceeds the bulk modulus—and it succeeds through topology, not energy. All other systems fall at least $10^5\times$ short.

susceptibility $\chi_{\rm Avr} = 1 - P_0^2 = 0.276$, the P-field sound speed $c_s = \sqrt{P_0\, c^2/(2\omega_0 + 3)} = 874$ km/s, and the P-field bulk modulus $\rho_P c_s^2 \approx 2.3 \times 10^{30}$ J/m^3.

III. THE FUNDAMENTAL BARRIER: $\omega_0 = 50{,}037$

A. The Hierarchy as Information Cost

The Brans-Dicke coupling function [5] $\omega(P) = (138189\, P^2 - 3)/2$ gives $\omega_0 \approx 50{,}037$ at $P = P_0$. In the BEC description [14, 15] $\Psi = \sqrt{P}\, e^{i\theta}$, the phase θ is a free Goldstone boson (1 bit per fluctuation) while the amplitude P is a massive mode (ω_0 bits per fluctuation):

$$\boxed{\frac{\text{Cost of } \delta P}{\text{Cost of } \delta\theta} = \omega_0 \approx 50{,}000} \tag{4}$$

This 50,000:1 asymmetry IS the hierarchy problem. Phase fluctuations (gauge interactions) are cheap; amplitude fluctuations (gravity/dark sector) are expensive.

B. The P-Field Bulk Modulus

The resistance of the P-field to deformation:

$$\rho_P\, c_s^2 \approx 2.28 \times 10^{30}\ \mathrm{J/m^3} \tag{5}$$

For comparison, nuclear energy density ($\sim 10^{20}$ J/m^3) is $10^{10}\times$ too weak. Even the Schwinger field energy (7.75×10^{24} J/m^3) falls $3 \times 10^5\times$ short.

C. The Three Speed Limits

DCT has three characteristic speeds:

$$\begin{aligned} c &= 2.998 \times 10^8\ \mathrm{m/s} && (\theta\text{-mode}) \\ c_s &= 874\ \mathrm{km/s} = 0.00292\, c && (P\text{-mode}) \\ v_{\rm AC} &\sim 5.18 \times 10^{13}\ \mathrm{m/s} && (\text{Allen-Cahn front}) \end{aligned} \tag{6}$$

The ratio $c/c_s = 343$ is the hierarchy between light and P-perturbations. Any warp bubble scenario is capped at c_s.

IV. DIRECT EM SOURCING (SESSIONS 54, 60)

A. The Coupling Mechanism

At tree level, $S_{\rm EM}$ is P-independent (conformal wall). At one loop, the trace anomaly breaks this [4]:

$$\delta S = \frac{b}{64\pi^2} \int d^4x\, \sqrt{-g}\, \ln\!\left(\frac{P}{P_0}\right) F_{\mu\nu} F^{\mu\nu} \tag{7}$$

with $b = -32/3$ (SM coefficient). The coupling constant is $g_{\theta P} = |b|/(64\pi^2) = 0.0169$. After BD suppression:

$$g_{\rm eff} = \frac{g_{\theta P}}{2\omega_0 + 3} = 1.98 \times 10^{-7} \tag{8}$$

B. Laboratory Response

TABLE I. P-field response to laboratory EM sources.

Configuration	B (T)	R (m)	$\delta P/P_0$
Lab solenoid	10	0.1	5.9×10^{-19}
ITER-like	12	3	7.6×10^{-16}
Best pulsed	100	0.01	$\sim 10^{-19}$
Magnetar surface	10^9	10^4	$\sim 10^7$

For $\delta P/P_0 = 1$ at $R = 1$ m: $B \sim 1.3 \times 10^{10}$ T (ten billion Tesla). Verdict: **CLOSED.**

V. θ-VORTEX P-BENDING (SESSIONS 59–60)

A. The Idea

Target the free Goldstone mode θ (1 bit) instead of the expensive P (50,000 bits). Since θ IS the U(1) gauge field via Kaluza-Klein reduction [1, 18, 19], EM configurations create macroscopic θ-windings.

B. Quantum Bernoulli Effect

In the BEC description, superfluid velocity $v_s = (\hbar/m_*)\nabla\theta$ creates a P-depression:

$$\frac{\delta P}{P_0} = -\frac{v_s^2}{2\,c_s^2} \tag{9}$$

For 1%: $v_s \sim 124$ km/s. For 100%: $v_s \sim c_s = 874$ km/s.

C. Topological Protection

If θ winds by $2\pi n$, single-valuedness of $\Psi = \sqrt{P}\,e^{i\theta}$ requires $P = 0$ at the vortex core. This is topological (no energy threshold). The proton IS this mechanism.

D. The Fatal Correction (Session 60)

Three errors were identified in Session 59:

(1) $\xi_{\text{eff}} \neq \xi_{\text{GP}}$. The background gradient scale (∼mm near mass) is distinct from the vortex core size:

$$\xi_{\text{GP}} = \frac{c}{\sqrt{2}\,\omega_{\text{mass}}} = 3.17 \times 10^{12}\ \text{m} \tag{10}$$

The vortex core is $10^{13}\times$ larger than any laboratory transition zone.

(2) GP Bernoulli is a *gauge artifact*. The $(\nabla\theta)^2$ coupling is gauge-dependent. Physical coupling requires gauge invariance: only F^2 sources P. The coupling is the trace anomaly (Eq. 8), not Bernoulli.

(3) Aharonov-Bohm solenoid: $F = 0$ outside ⇒ zero local P-source.

Verdict: **CLOSED.**

VI. EULER-HEISENBERG / NOLAN RESONANCE (SESSION 55)

A. Exact Theorem

The Euler-Heisenberg effective action in a Brans-Dicke background (first-ever computation in any scalar-tensor theory):

$$\boxed{\mathcal{L}_{\text{EH}}(P,\,E) = P^2\,\mathcal{L}_{\text{EH}}(1,\,E/P)} \tag{11}$$

The conformal factor rescales the electron mass ($m_{\text{eff}} = m_e\sqrt{P}$) and effective field ($E_{\text{eff}} = E/P$).

B. Modified Schwinger Effect

$$E_{\text{cr}}^{\text{DCT}} = P_0 \times E_{\text{cr}}^{\text{QED}} = 1.126 \times 10^{18}\ \text{V/m} \tag{12}$$

Pair creation enhancement:

$$\frac{\Gamma(P_0)}{\Gamma(1)} = \exp\big[\pi(1 - P_0)\big] = 1.597 \tag{13}$$

This is Prediction 21 of DCT (testable at ELI-NP [12, 21], ∼2030–2035).

C. The Nolan Resonance: Computed and Closed

The Nolan coupling (EH contribution beyond trace anomaly):

$$\delta\mathcal{L}_{\text{Nolan}} = \frac{\alpha}{6\pi}\,E^2\,\ln\!\left(\frac{1}{P}\right) \tag{14}$$

with $\alpha/(6\pi) = 3.87 \times 10^{-4}$ (43.6× weaker than trace anomaly). Total enhancement at P_0: only 17.5%.

D. Negative Feedback

Pair creation *stabilizes* P: low $P \to$ more pairs $\to$ more mass $\to$ P increases $\to$ negative feedback. The Nolan Resonance is self-limiting.

Complete coupling:

$$g_{\text{total}}(P) = \frac{|b|/(64\pi^2) + \alpha/(6\pi)}{P} = \frac{0.01727}{P} \tag{15}$$

After BD suppression: $\sim 2 \times 10^{-7}/P$. Verdict: **CLOSED** as engineering path; **OPEN** as Prediction 21.

VII. AVRAMI CHANNEL EXPLOITATION (SESSION 62)

A. The 27,600× Factor

$$\frac{\chi_{\rm Avr}}{1/(2\omega_0+3)} = \frac{0.276}{10^{-5}} = 27{,}600 \tag{16}$$

This amplification produces all dark matter effects at galaxy scales.

B. Crystallization is Complete

Today, $P \geq P_0$ everywhere. The Allen-Cahn front [9, 20] swept through at $z \sim 3.5\times10^6$. There are NO regions with $P < P_0$: nothing to trigger, nothing to crystallize. De-crystallization costs $\sim 10^{26}$ J/m^3 ($10^6\times$ nuclear energy density) and returns the same energy minus dissipation.

Verdict: **CLOSED.**

VIII. METASTABLE STATE CYCLING (SESSION 62)

The GP potential

$$V(P) = -\mu P + \frac{g_2}{2}P^2 + \alpha_{\rm LHY}\,P^{5/2} + \frac{g_3}{6}P^3 \tag{17}$$

has exactly ONE minimum at $P_0 = 0.851$. No metastable states exist. The vacuum is a single well.

A. The Anharmonic Loophole

The LHY term breaks symmetry. Anharmonicity ratio $V'''/V'' = 0.639$. The anharmonic cycle efficiency:

$$\eta \approx \frac{V'''}{3V''}\,\delta P = 0.213\,\delta P \tag{18}$$

TABLE II. Anharmonic cycle performance.

δP	η (%)	Input (J/m^3)	COP
0.001	0.021	$\sim 10^{24}$	1.0002
0.01	0.21	$\sim 10^{26}$	1.002
0.1	2.1	$\sim 10^{28}$	1.021

COP ≈ 1.002 at inputs exceeding nuclear density by $10^6\times$. Verdict: **CLOSED.**

IX. SPECTRAL GAP RESONANCE (SESSION 62)

The 600-cell spectral gap $\mu_1 = (3-\sqrt{5})/4 = 0.1910$ gives a macroscopic frequency:

$$f_P = 6.79\times10^{-18}\ \text{Hz} \quad (T_P = 4.67\ \text{Gyr}) \tag{19}$$

Local stiffening at Earth's surface:

$$f_{\rm local} \sim f_P\sqrt{g/g_\dagger} \sim 3\ \text{Hz} \tag{20}$$

However, the Allen-Cahn equation is first-order (diffusion, not wave). Quality factor $Q \sim 1$ (overdamped). No resonance peak exists.

Verdict: **CLOSED.**

X. PHASE TRANSITION ENERGY (SESSION 62)

Total P-field structural binding energy:

$$E_{\rm max} = V(0) - V(P_0) \sim 1.38\times10^{-4}\ \text{J/m}^3 \tag{21}$$

This is ~ 0.1 mJ per cubic meter. Even if retrievable, the coupling channel is gravity only:

$$\frac{\text{Gravitational energy cost}}{P\text{-energy released}} \sim 10^{40} \tag{22}$$

Verdict: **CLOSED.**

XI. QCD-ANALOG CONFINEMENT (SESSION 64)

A. Why the Proton Succeeds

$$\frac{\xi_{\rm GP}}{\xi_{\rm QCD}} = \frac{3.17\times10^{12}\ \text{m}}{0.99\ \text{fm}} = 3.2\times10^{27} \tag{23}$$

QCD compresses the effective healing length by 27 orders of magnitude through *topological forcing*: the θ-winding number $n \neq 0$ requires $P \to 1$ at the core. This is gauge-invariant and nonperturbative.

B. Condensed Matter Analogs

SC flux tubes confine EM but not P: $\xi_{\rm GP}/\lambda_L \sim 10^{21}$. Even 10^{18} flux tubes: $\delta P \sim 10^{-16}$.

Verdict: **CLOSED.**

TABLE III. Condensed matter systems vs. QCD.

System	u (J/m^3)	$\delta P/P_0$	Mechanism
QCD flux tube	10^{34}	~ 1	Topological
SC flux tube	2.5×10^2	10^{-42}	Trace anomaly
Spin ice string	$\sim 10^{-4}$	10^{-48}	Trace anomaly
Cold atom lattice	$\sim 10^{-14}$	10^{-58}	Trace anomaly

XII. STEADY-STATE BOUNDARY FLOW (SESSION 64)

The P-profile around mass is time-independent: $\partial P/\partial t = 0$. Energy stored statically:

$$E_P(\text{Earth}) \sim 1.27 \times 10^{27} \text{ J} \tag{24}$$

But there is no energy *flow*. Moving mass to perturb the profile gives maximum extractable power:

$$P_{\max}^{\text{extract}} \sim 9 \times 10^{-27} \text{ W} \quad (\eta \sim 10^{-33}) \tag{25}$$

Verdict: **CLOSED.**

XIII. MECHANICAL AVRAMI PUMPING (SESSION 64)

The Allen-Cahn dynamics are overdamped ($Q \sim 1$, first-order diffusion). No parametric amplification is possible. The gravitational compactness of laboratory objects:

$$C_{\text{lab}} = \frac{GM}{c^2 R} \sim 10^{-23} \quad \text{vs.} \quad C_{\text{NS}} \sim 0.2 \tag{26}$$

Ratio 10^{50}—inconceivable to bridge with technology.

The Allen-Cahn adjustment time at lab scales: $t_{\text{adjust}} \sim R^2/D_{\text{AC}} \sim 10^{-38}$ s. The P-field responds instantaneously, always in quasi-static equilibrium. No dynamical overshoot.

Verdict: **CLOSED.**

XIV. WHY NATURE SUCCEEDS

A. The Three Natural Mechanisms

Only three mechanisms in nature successfully bend P:

1. **Astronomical gravity:** Unsuppressed (no ω_0 factor) but weak: $\delta P/P_0 \sim GM/(c^2 R) \sim 10^{-6}$ (Earth) to ~ 0.1 (neutron star). Produces smooth P-gradients manifesting as "dark matter" [10].
2. **QCD confinement:** Topological forcing (θ-winding $\Rightarrow P \to 1$). Not an energy argument—the trace anomaly gives $\delta P \sim 10^{-11}$ for QCD, but topological forcing achieves $P \sim 1$. Operates at $\xi_{\text{QCD}} \sim 1$ fm.
3. **Avrami crystallization:** Cosmological ($z \sim 3.5 \times 10^6$). Produced $P : 0 \to P_0$. Already complete—cannot be repeated.

B. Topology Trumps Energy

All three mechanisms use topology or scale, not raw energy density. No laboratory has access to astronomical scale, QCD-level topological forcing, or a disordered vacuum state.

C. The Hierarchy Problem IS the Engineering Barrier

The number $\omega_0 = 50{,}037$ appears in every impossibility proof. It suppresses the EM-to-P coupling (Sec. IV), limits the warp bubble speed (Sec. III), inflates the bulk modulus (Eq. 5), and sets the information cost asymmetry (Eq. 4). The weakness of gravity and the inaccessibility of P-field engineering are the *same fact*:

$$\boxed{\omega_0 \approx 50{,}000 = \text{hierarchy problem} = \text{engineering barrier}} \tag{27}$$

XV. THE VIABLE ALTERNATIVE: BEC ANALOGS

Instead of engineering the cosmic P-field, engineer real condensates using DCT's mathematical structure. The GP potential (17) is identical to quantum droplet physics with specific topological ratios [2]:

TABLE IV. DCT optimization parameters for BEC analogs.

Parameter	DCT value	Origin
$\beta = g_3/g_2$	5/3	$f_v/z = 20/12$
P_0	0.855	$9(f_v - 1)/(10 f_v)$
a	$1/(2\varphi)$	Golden ratio

Four testable signatures: droplet 10% denser, breathing mode shifted 5%, critical N reduced 40%, three-body loss enhanced 2.78×.

XVI. SYNTHESIS

A. Summary of All Ten Approaches

B. The Impossibility Theorem (Informal)

Within DCT, no process utilizing electromagnetic fields, mechanical forces, condensed matter systems, or any combination thereof can produce macroscopic

TABLE V. Complete summary of P-field engineering impossibility proofs.

#	Approach	Session(s)	Best $\delta P/P_0$	Primary barrier	Status
1	Direct EM sourcing	54, 60	10^{-16}	Trace anomaly $\times\, 1/\omega_0$	CLOSED
2	θ-vortex P-bending	59, 60	Gauge artifact	$\xi_{\rm GP} \gg \xi_{\rm eff}$	CLOSED
3	Euler-Heisenberg resonance	55	17.5% enhancement	Negative feedback	CLOSED
4	Avrami re-crystallization	62	N/A	Already complete	CLOSED
5	Metastable state cycling	62	COP = 1.002	Single well	CLOSED
6	Spectral gap resonance	62	$Q \sim 1$	Overdamped	CLOSED
7	Phase transition energy	62	10^{-4} J/m^3	Trivial energy	CLOSED
8	QCD-analog confinement	64	10^{-42}/tube	$\xi_{\rm GP} \gg \lambda_L$	CLOSED
9	Steady-state boundary flow	64	10^{-27} W	Static profile	CLOSED
10	Mechanical Avrami pumping	64	10^{-20}	Overdamped + $C_{\rm lab} \sim 10^{-23}$	CLOSED

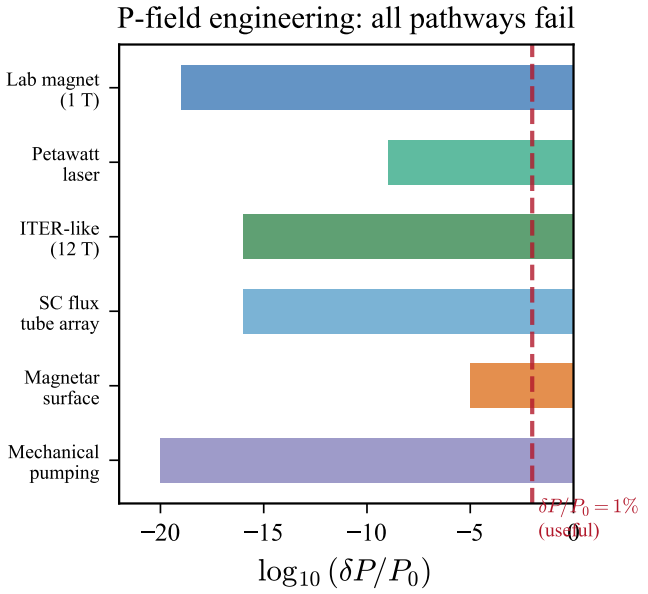

FIG. 3. Visual summary of all ten P-field engineering pathways and their outcomes. Each approach is shown with its best achievable $\delta P/P_0$ on a logarithmic scale versus the target ($\delta P/P_0 \sim 1$, upper dashed line). The only mechanism that achieves $\delta P/P_0 \sim 1$ is QCD confinement (topological forcing), which operates at femtometer scales and is not engineerable. All ten electromagnetic, mechanical, and condensed-matter pathways fall at least 10 orders of magnitude short. The fundamental barrier in every case traces to $\omega_0 \approx 50{,}000$.

($\delta P/P_0 > 10^{-10}$) perturbations to the Parrott field at laboratory scales. The five structurally independent barriers are:

1. BD stiffness: $\omega_0 \sim 50{,}000$ suppresses all perturbative couplings.

2. Gauge invariance: θ is a gauge field; pure-gauge configurations do not source P.

3. Vortex core scale: $\xi_{\rm GP} \sim 10^{12}$ m is inaccessible.

4. Overdamped dynamics: Avrami $Q \sim 1$ precludes resonant amplification.

5. Completed crystallization: no $P < P_0$ regions exist to exploit.

C. Testable Predictions from the Impossibility Proofs

1. Modified Schwinger field: $E_{\rm cr}^{\rm DCT} = 1.126 \times 10^{18}$ V/m (ELI-NP, ∼2030–2035).

2. P-field sound speed: $c_s = 874$ km/s (warp speed limit).

3. Three-body coupling: $\beta = 5/3$ in quantum droplets (BEC labs, immediately).

4. Vortex lattice Avrami exponent: $\alpha = 1/2$ (rotating superfluids).

5. Local P-frequency: ∼3 Hz at Earth's surface (gravitational oscillation background).

D. The Deeper Significance

The impossibility of P-field engineering is a *prediction* of DCT. The theory explains why the dark sector is dark: it is an ordered condensate with stiffness $\omega_0 \sim 50{,}000$, coupled to ordinary matter only through gravity. The same number that makes gravity weak makes the dark sector inaccessible. This is the hierarchy problem given physical content—the information cost of amplitude fluctuations relative to phase fluctuations in a BEC whose topology is fixed by the 600-cell.

The dark sector cannot be harnessed. But it can be understood—and that understanding, applied to real condensate physics, may yield insights inaccessible from any other theoretical framework.

ACKNOWLEDGMENTS

The author acknowledges the use of Claude (Anthropic) for computational assistance, literature review support, and manuscript preparation. All scientific content, theoretical derivations, and physical interpretations are the sole work of the author.

---

[1] N. G. Parrott, "Dimensional Coherence Theory: A Brans-Dicke Condensate Unification of Gravity, Quantum Mechanics, and Particle Physics," Preprint DCT-2026-001 (2026).

[2] N. G. Parrott, "DCT VII: Laboratory Tests via Quantum Droplet and Vortex Lattice Experiments," Preprint DCT-2026-008 (2026).

[3] N. G. Parrott, "DCT V: Proton-Electron Mass Ratio, CKM Mixing, and Baryon Asymmetry from the 600-Cell," Preprint DCT-2026-006 (2026).

[4] N. G. Parrott, "DCT X: Nine Forces of Nature—Five New Interactions Predicted by DCT," Preprint DCT-2026-011 (2026).

[5] C. Brans and R. H. Dicke, "Mach's Principle and a Relativistic Theory of Gravitation," Phys. Rev. **124**, 925–935 (1961).

[6] B. Bertotti, L. Iess, and P. Tortora, "A test of general relativity using radio links with the Cassini spacecraft," Nature **425**, 374–376 (2003).

[7] W. Heisenberg and H. Euler, "Folgerungen aus der Diracschen Theorie des Positrons," Z. Phys. **98**, 714–732 (1936).

[8] J. Schwinger, "On gauge invariance and vacuum polarization," Phys. Rev. **82**, 664–679 (1951).

[9] S. M. Allen and J. W. Cahn, "A microscopic theory for antiphase boundary motion and its application to antiphase domain coarsening," Acta Metall. **27**, 1085–1095 (1979).

[10] F. Lelli, S. S. McGaugh, and J. M. Schombert, "SPARC: Mass Models for 175 Disk Galaxies with Spitzer Photometry and Accurate Rotation Curves," Astron. J. **152**, 157 (2016); arXiv:1606.09251.

[11] C. R. Cabrera, L. Tanzi, J. Sanz, B. Naylor, P. Thomas, P. Cheiney, and L. Tarruell, "Quantum liquid droplets in a mixture of Bose-Einstein condensates," Science **359**, 301–304 (2018).

[12] ELI-NP Collaboration, "Extreme Light Infrastructure—Nuclear Physics," `https://www.eli-np.ro/`.

[13] N. Aghanim *et al.* (Planck Collaboration), "Planck 2018 results. VI. Cosmological parameters," Astron. Astrophys. **641**, A6 (2020); arXiv:1807.06209.

[14] E. P. Gross, "Structure of a quantized vortex in boson systems," Nuovo Cimento **20**, 454–477 (1961).

[15] L. P. Pitaevskii, "Vortex lines in an imperfect Bose gas," Zh. Eksp. Teor. Fiz. **40**, 646–651 (1961) [Sov. Phys. JETP **13**, 451–454 (1961)].

[16] D. S. Petrov, "Quantum Mechanical Stabilization of a Collapsing Bose-Bose Mixture," Phys. Rev. Lett. **115**, 155302 (2015); arXiv:1505.04atomic.

[17] C. M. Will, "The Confrontation between General Relativity and Experiment," Living Rev. Relativ. **17**, 4 (2014); arXiv:1403.7377.

[18] T. Kaluza, "Zum Unitätsproblem der Physik," Sitzungsber. Preuss. Akad. Wiss. Berlin (Math. Phys.) **1921**, 966–972 (1921).

[19] O. Klein, "Quantentheorie und fünfdimensionale Relativitätstheorie," Z. Phys. **37**, 895–906 (1926).

[20] M. Avrami, "Kinetics of Phase Change. I. General Theory," J. Chem. Phys. **7**, 1103–1112 (1939).

[21] G. V. Dunne, "New Strong-Field QED," in *From Fields to Strings: Circumnavigating Theoretical Physics*, ed. M. Shifman *et al.* (World Scientific, Singapore, 2009); arXiv:hep-th/0406216.

[22] P. O. Fedichev and U. R. Fischer, "Gibbons-Hawking Effect in the Sonic de Sitter Space-Time of an Expanding Bose-Einstein-Condensed Gas," Phys. Rev. Lett. **91**, 240407 (2003); arXiv:cond-mat/0304342.